

A Novel Experimental Device for Seebeck Coefficient Measurements of Bulk Materials, Thin Films, and Nanowire Composites

D. Pinisetty

Department of Mechanical Engineering,
Louisiana State University,
Baton Rouge, LA 70803

N. Haldolaarachchige

D. P. Young

Physics and Astronomy,
Louisiana State University,
Baton Rouge, LA 70803

R. V. Devireddy¹

Department of Mechanical Engineering,
Louisiana State University,
Baton Rouge, LA 70803
e-mail: devireddy@me.lsu.edu

An experimental setup has been designed and built for measuring the Seebeck coefficient of bulk thermoelectric materials, thin films, and nanowire composites in the temperature range 200–350 K. The setup utilizes a differential method for measuring the Seebeck coefficient of the sample. The sample holder is a simple clamp design, utilizing a spring-loaded mounting system to load and hold the sample between two copper blocks, on which the electrical leads, as well as thermocouples, are mounted. The spring-loaded design also offers fast turn-around times, as the samples can be quickly loaded and unloaded. To measure the Seebeck coefficient, a temperature difference is generated across the sample by using four 10 k Ω resistive heaters mounted in series on one of the copper blocks. The resulting slope of the thermo-emf versus temperature difference plot is used to obtain the Seebeck coefficient at any temperature. Test measurements were carried out on bulk samples of nickel (Ni), bismuth-telluride (Bi₂Te₃), antimony-telluride (Sb₂Te₃), as well as thin films and nanowire composites of Ni. [DOI: 10.1115/1.4003192]

Keywords: thermoelectricity, bismuth-telluride, antimony-telluride, nickel, electrodeposition, physical property measurement system, differential method

1 Introduction

Recently a great deal of scientific and technological interest has been focused on the production of highly efficient thermoelectric materials because of their fundamental importance and potential applications, such as electronic devices, nonconventional energy sources, etc. [1–3]. Both bulk materials and low dimensional materials have been explored, and their thermoelectric performance is determined by the dimensionless thermoelectric figure of merit (ZT), where $ZT = (S^2T)/(\rho\kappa)$. Here, S is the Seebeck coefficient, T is temperature, ρ is the absolute electrical resistivity, and κ is the thermal conductivity. In evaluating ZT it is essential to measure the key transport properties: S , ρ , and κ . Reliable and accurate measurement of the Seebeck coefficient is absolutely essential to evaluate the potential of materials for thermoelectric applications. Seebeck coefficient measurements also yield important information about the nature of charge carriers, phase transformation, defect chemistry, etc. [4].

The two basic experimental techniques for measuring the Seebeck coefficient are the integral method and the differential method [5]. In the differential method, which is often used to measure the Seebeck coefficient of semiconductors [5], the thermo-emf (ΔV) generated is plotted against a small thermal gradient (ΔT). The slope of ΔV versus ΔT gives the Seebeck coefficient. Experimental techniques measuring the Seebeck coefficient based on the differential method have been well covered in literature. Early studies by Testardi and McConnell [6] and Cowles and Dauncey [7] have suggested measuring the Seebeck coefficient using Chromel-Alumel thermocouple wires. Cowles and Dauncey [7] reported the measurement of the Seebeck coefficient at room

temperature using a direct potentiometer circuit. The circuit used in their study yielded the differential Seebeck coefficient of the specimen with respect to the copper probe, as compared with Chromel-Alumel thermocouples held at the same temperature gradient. Later, Wood et al. [8] developed a high temperature (1900 K) apparatus for measuring Seebeck coefficients of bulk specimens. In their setup the temperature gradient was created by using light pulses transmitted via light pipes. Caskey et al. [9] then came up with a new technique for rapid measurement of the Seebeck coefficient for rod shaped specimens over a wide temperature range (4.2–300 K). The technique developed by Caskey et al. [9] simultaneously measures ΔT and ΔV as the temperature gradient is slowly increased. Chaussy et al. [10] designed a cryogenic system to measure thermopower, thermal conductivity, and electrical resistivity of bulk materials, simultaneously over a wide range of temperature between 1.2 K and 350 K. Gee and Green [11] developed an apparatus to measure the Seebeck coefficient of thick uniform disks and thin films down to 100 nm thickness. The probes employed in the apparatus were smaller than the ones employed by Cowles and Dauncey [7]. Smaller probes make the design suitable for incorporation into low temperature cryostats. Although the apparatus developed by Gee and Green [11] facilitates Seebeck coefficient measurements at room temperature and below room temperature for both bulk materials and thin films, the electrical contact between the thermocouple and hot probe may lead to spurious results. To improve on this design, Goldsmid [12] came up with a modified apparatus of Cowles and Dauncey [7] using a simplified circuit and isolating the thermocouple wires from the probe and heat sink. However, the simplified apparatus of Goldsmid [12] requires specific resistors to obtain the desired sensitivity over only a limited range of Seebeck coefficients. Platzek et al. [13] developed a scanning Seebeck microprobe combined with measurement of electric potential along the surface of bulk materials. By mounting the probe to a three dimensional

¹Corresponding author.

Manuscript received October 21, 2010; final manuscript received December 3, 2010; published online February 4, 2011. Editor: Vijay K. Varadan.

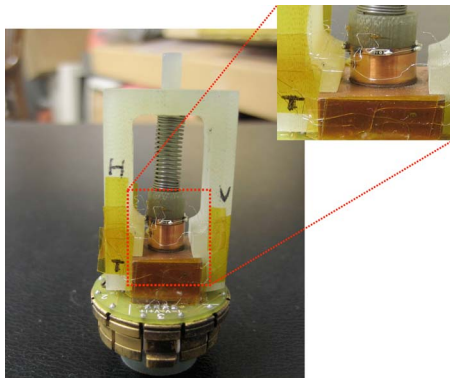


Fig. 1 A photograph of the measurement setup mounted on a PPMS puck. The sample is mounted between two copper blocks, one of which acts as a heater and the other acts as a heat sink.

micropositioning system they determined the spatial variation of the Seebeck coefficient. Studies [4,14–16] focused on the measurement of the Seebeck coefficient and electrical resistivity of bulk materials over a wide range of temperature using a variety of designs have been well covered in literature. The theoretical predictions and experimental studies of Dresselhaus and co-workers [17–20], that the reduction in dimensionality enhances the thermoelectric efficiency when compared with bulk materials, have since stimulated scientists to focus on the measurement of Seebeck coefficients of thin films and nanomaterials.

Burkov et al. [21] described an experimental setup for the measurement of the Seebeck coefficient and electrical resistivity of bulk materials and thin films for a wide range of temperatures (100–1300 K). Later, Boffoue et al. [22] developed a fully automated experimental setup for Seebeck coefficient and electrical resistivity measurements for both bulk materials and thin films within a temperature range 77–330 K. The setup developed by Boffoue et al. [22] had a combination of accuracy, rapidity, easy sample mounting, and greater flexibility with changes in the geometrical dimensions of the sample. Recently, Sarath Kumar and Kasiviswanathan [23] reported an experimental setup (using integral method) for the measurement of the Seebeck coefficient of thin wires and thin films in the temperature range 300–650 K.

In the present study, we describe an apparatus designed to measure the Seebeck coefficient within a temperature range 120–350 K on bulk materials, thin films, and nanowire composites. The sample holder has been designed to fit inside a commercial cryostat—the physical property measurement system (PPMS) manufactured by Quantum Design. The PPMS sample holder consists of a small, round, “puck,” which fits down inside the cryostat. Our Seebeck sample holder has been built on top of this puck. The uniqueness of our apparatus is the relative ease with which samples can be changed, as well as the extremely accurate temperature control afforded by the PPMS system. The Seebeck coefficient measurements were made using the differential method (slope of ΔV versus ΔT). In testing the apparatus, the Seebeck coefficients of bulk samples of bismuth-telluride, antimony-telluride, and nickel were measured. To prove the flexibility of the device, test measurements were also carried out on nickel thin films and nickel nanowire composites.

2 Apparatus Description

A photograph snapshot of the apparatus mounted on a PPMS puck is shown in Fig. 1. The entire setup is constrained to 5 cm in height with an 11×13 mm² footprint. To ensure good thermal contact between the sample and the temperature sensors, highly conductive (oxygen free high conductive copper (OFHC)) copper rods are used to sandwich the sample between them. Using silver

epoxy (Epotek H20E), differential thermocouples are attached firmly and securely to the copper rods. Four resistive heaters are connected in series and are firmly attached on the circumference of the upper copper rod acting as a heater. A spring-loaded mechanism is employed on the top of the heated copper probe. The force exerted can be finely adjusted and the sample can be squeezed between the copper rods to ensure good thermal contact. The force will be constant during the entire experiments due to spring loading. A support housing made of G-10/FR-4 is supported by screws and fixed onto the heat sink (copper base) to add rigidity to the setup.

3 Experimental Procedures

3.1 Preparation of Bulk Samples. Bulk samples of nickel (Ni), bismuth-telluride (Bi_2Te_3), and antimony-telluride (Sb_2Te_3) were prepared in the form of pressed pellets [24]. Stoichiometric amounts of the powders of starting materials are mixed and ground well in an alumina mortar. The mixture is then pressed into pellets of 5 mm diameter under 635 MPa pressure using a stainless steel Graseby Specac die and hydraulic press. In the case of bismuth-telluride (Bi_2Te_3) and antimony-telluride (Sb_2Te_3), bulk samples are further prepared by RF induction melting [25]. The sample is placed in an alumina crucible, which is wrapped with a thin tantalum foil susceptor. The crucible and susceptor are then heated inside an induction coil furnace under ultrahigh-purity argon gas. RF induction heating provides reliable, repeatable, non-contact, and energy-efficient heat in a minimal amount of time. The charge can be melted and then maintained in the liquid state indefinitely, depending on the application requirements. The operating frequency of the RF supply is 0–100 kHz.

3.2 Preparation of Thin Film Samples. Thin film samples of Ni were prepared by an electroplating technique. The electroplating bath consisted of nickel sulfamate (89 g/l), boric acid (45 g/l), wetting agent (0.3% vol/l), and de-ionized (DI) water. Electroplating was performed at a current density of 10 mA/cm² on a silicon wafer sputtered with gold. The deposited film after a deposition time of 1 h was mechanically separated from the wafer and used for the Seebeck coefficient measurement.

3.3 Preparation of Nanowire Composites. Nanowire composite samples of Ni were fabricated by electrodeposition [26–39]. Electrodeposition was carried out in a typical three-electrode setup. Polycarbonate (PC), (Poretics PCTE, GE Osmonics, Minnetonka, MN) nanoporous membrane filters were sputter coated with gold on one side and used as a working electrode. The manufacturer specified average pore diameter of the PC membrane was ~ 100 nm, while the thickness was 8 μm . The gold surface was kept in contact with a copper plate held inside a polyetheretherketone (PEEK) stationary holder, and a circular area of 2 cm² was exposed to the electrolyte for electrodeposition. A platinum mesh used as a counterelectrode was placed above the working electrode. Both the counter- and working electrodes were held horizontal in the electrolyte. An Acumet saturated calomel reference electrode (SCE) was used to record the potential at the working electrode. The reaction cell consisted of a 1000 ml beaker, filled with nickel sulfamate (89 g/l), boric acid (45 g/l), wetting agent (0.3% vol/l), and DI water, which acts as an electrolyte. The reaction cell was kept inside a water bath maintained at a temperature of $50 \pm 2^\circ\text{C}$, and the electrolyte was magnetically stirred at 320 rpm during the experiments. All the experiments were carried out with a VersaSTAT3 potentiostat/galvanostat (AMETEK Princeton Applied Research, TN). The Ni nanowires were galvanostatically deposited at a cathodic current density of 5 mA/cm² by using a template-based synthesis technique [40,41] in which an appropriate current was applied to the solution causing the metal to deposit within the pores of the gold-sputtered membrane. After deposition, the membrane was dissolved in methylene chloride (CH_2Cl_2) and sonicated for 30 min to release the

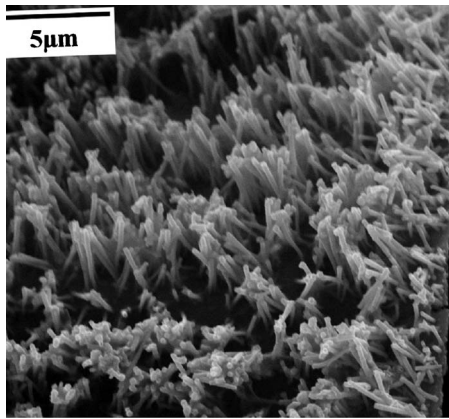


Fig. 2 SEM image of Ni nanowire arrays electrodeposited at $\sim 6 \text{ mA cm}^{-2}$ using a PC template with an average pore diameter of $\sim 100 \text{ nm}$ and an average length of $6 \text{ }\mu\text{m}$

nanowires. Scanning electron microscopy (SEM) images of the nanowires were obtained using a JEOL 840A electron microscope

3.4 Seebeck Coefficient Measurement Procedure. In order to perform measurements at different temperatures, the Seebeck apparatus is placed on a PPMS puck and inserted into the PPMS system. A custom designed temperature control and measurement program, created with LABVIEW software operating on a Dell PC, runs the experiment. Heater current is supplied by a Keithley 220 dc source, and the thermo-emf and differential thermocouple voltage are measured by Keithley 182 nanovoltmeters and recorded by the PC.

4 Results and Discussion

The bulk samples of Ni, Sb_2Te_3 , and Bi_2Te_3 were prepared as mentioned in Sec. 3. The Seebeck coefficient of these samples was then measured using the experimental setup described in the present study. All the measurements were performed on five different bulk samples for each material. To test the experimental setup for measurement of the Seebeck coefficient of nanowire array composite samples, Ni nanowires were fabricated using electrodeposition. The measurements for the nanowires were performed on three different electrodeposited samples. Figure 2 depicts the typical top view of the Ni nanowire arrays electrodeposited at a cathodic current density of $\sim 6 \text{ mA/cm}^2$ using a PC membrane with an average pore diameter of $\sim 100 \text{ nm}$. The nanowires have the same height, implying they are deposited along the pores at the same rate.

To demonstrate the accuracy of the measurement system Seebeck coefficient results of bulk semiconductors Sb_2Te_3 and Bi_2Te_3 are presented in Fig. 3. The Seebeck coefficient data of bulk Sb_2Te_3 (filled circles and the right y-axis) presented in Fig. 3(a) show that the data are positive in the whole temperature range investigated, and the values are in good agreement (uncertainty of $\pm 2 \text{ }\mu\text{V/K}$) with the values reported by Zhitinskaya et al. [42] along the trigonal crystal axis. Similarly, the Seebeck coefficient data of bulk Bi_2Te_3 presented in Fig. 3(a) (filled squares and the left y-axis) show that the data are negative in the whole temperature range investigated and the values are in good agreement (uncertainty of $\pm 5 \text{ }\mu\text{V/K}$) with the values reported by Lowhorn et al. [43]. Figure 3(b) depicts the comparison of the measurements obtained from the experimental setup described in the present study and published literature for bulk Sb_2Te_3 and Bi_2Te_3 samples [42,43]. In Fig. 3(b), the Seebeck coefficient data of bulk Bi_2Te_3 obtained from the present study (dashed line) are compared with Ref. [43] (filled squares); most of the values are in agreement ($\pm 5 \text{ }\mu\text{V/K}$). The Seebeck coefficient data of bulk Sb_2Te_3 ob-

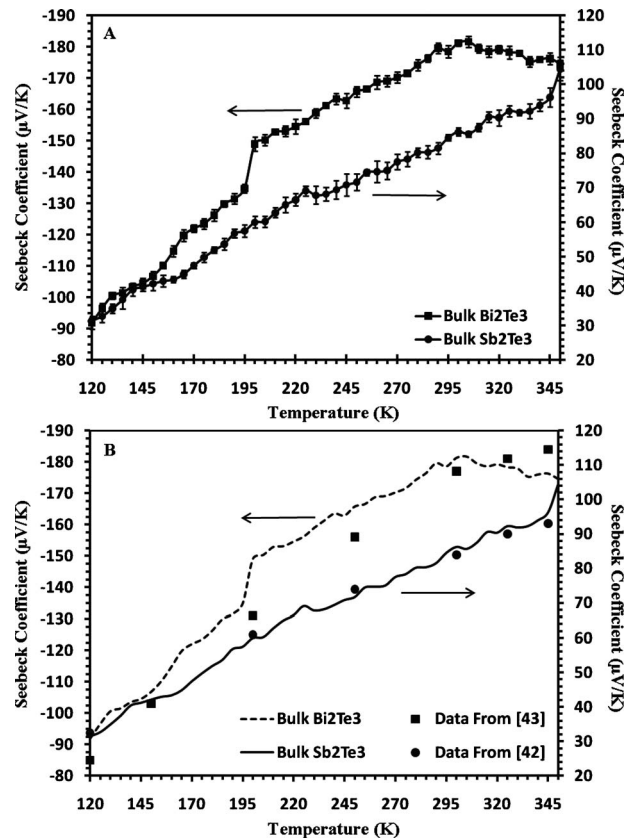


Fig. 3 (a) Temperature dependence of Seebeck coefficient ($\mu\text{V/K}$) measured (using the experimental setup described in the article) on a Sb_2Te_3 bulk sample (filled circles) and Bi_2Te_3 bulk sample (filled squares). (b) Temperature dependence of Seebeck coefficient ($\mu\text{V/K}$) measured using the experimental setup described in the article, of Bi_2Te_3 bulk sample (dashed line) and Sb_2Te_3 bulk sample (solid line), is compared with the values in the published literature, i.e., Ref. [43] for bulk Bi_2Te_3 and Ref. [42] for bulk Sb_2Te_3 samples.

tained from the present study (solid line) are compared with Ref. [42] (filled circles), and are in very close agreement with each other ($\pm 2 \text{ }\mu\text{V/K}$).

In order to validate the measurement system and estimate the accuracy involved in the data, Seebeck coefficient measurements were also performed on a bulk sample of nickel. Nickel was chosen as an appropriate test material, due to its relatively large Seebeck coefficient ($\sim 20 \text{ }\mu\text{V/K}$) among metals. The experimental data collected for bulk Ni samples within a temperature range 120–350 K are represented by filled circles in Fig. 4(a). To further test the capability of the measurement system on thin films and nanowire array composite samples, Seebeck coefficient measurements were performed on Ni thin films and Ni nanowire array composites. The experimental data collected for Ni thin films and Ni nanowire array composite are represented by filled squares and filled triangles, respectively, in Fig. 4(a). Note that the absolute Seebeck coefficient values of the Ni nanowires were lower than that of Ni thin films and bulk Ni samples, throughout the measured temperature range.

Figure 4(b) depicts the comparison of the measurements obtained from the experimental setup described in the present study and in published literature for bulk Ni and Ni nanowires [22,44–46]. In Fig. 4(b), the Seebeck coefficient data of Ni bulk sample obtained from the present study (shown as a solid line) are compared with experimental values obtained from Ref. [22] (shown as filled circles). The agreement between the Seebeck coefficient results of bulk Ni sample obtained in the present study

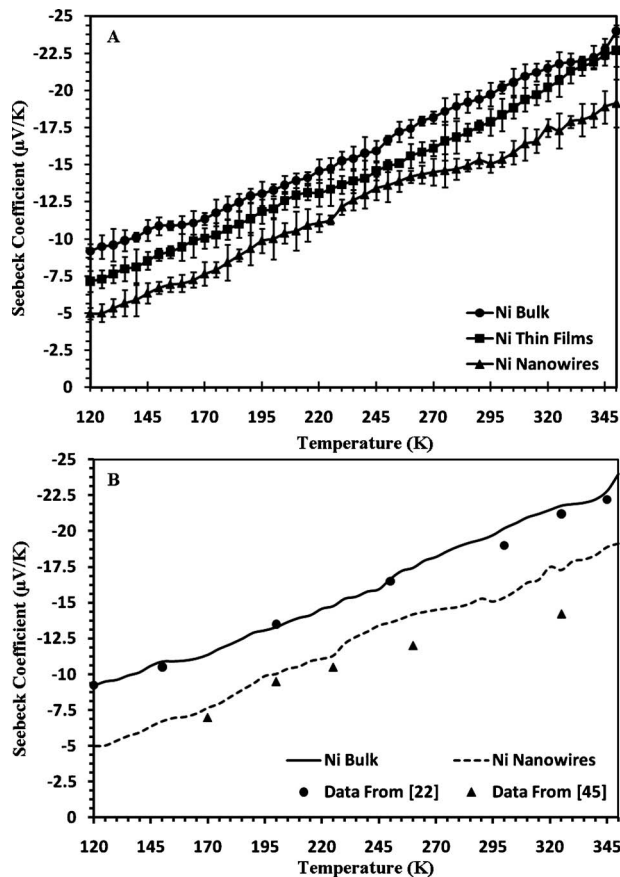


Fig. 4 (a) Temperature dependence of Seebeck coefficient ($\mu\text{V/K}$) measured (using the experimental setup described in the article) on a bulk Ni sample (filled circles), Ni thin film sample (filled squares), and a Ni nanowire array (filled triangles). (b) Temperature dependence of Seebeck coefficient ($\mu\text{V/K}$) measured using the experimental setup described in the article, of Ni bulk sample (solid line) and Ni nanowires with a diameter of 100 nm (dashed line), is compared with the values in the published literature, i.e., Ref. [22] for bulk Ni and Ref. [45] for Ni nanowires of 30 nm in diameter.

and the literature data [44–46,21,22] is rather good with an estimated uncertainty of about $\pm 0.6 \mu\text{V/K}$ (Fig. 4(b)). The Seebeck coefficient data of Ni nanowires with a diameter of 100 nm obtained from the present study (shown as a dashed-dotted line) are compared with experimental values reported in Ref. [45] (shown as filled triangles). Shapira et al. [45] measured the Seebeck coefficient of an individual Ni nanowire with a diameter of 30 nm and reported that the absolute value of the Seebeck coefficient of a Ni nanowire was lower than that of the bulk sample of Ni. Although the results in the present study cannot be directly compared with the results of Shapira et al. [45], since we used an array of nanowires as opposed to a single nanowire, the observed trends in the measured Seebeck coefficient values are in good agreement. To the best of our knowledge Seebeck coefficient data for Ni thin films are not currently available in published literature for a direct comparison with our results.

5 Conclusions

The aim of this study was to design and fabricate an experimental setup on a PPMS puck that could measure the Seebeck coefficient using the PPMS. While we tested the device over a moderate temperature range, the experimental setup ultimately provides flexibility in the temperature range ($4 \text{ K} < T < 350 \text{ K}$), as well as in regard to the sample dimensions. The sample loading

is relatively easy, and good thermal contacts are achieved by employing a spring-loading mechanism. Seebeck coefficient measurements of bulk samples, thin film samples, and nanowire composites can be performed with the experimental setup described in the study. To demonstrate the capability of the experimental setup, Seebeck coefficient measurements of bulk Bi_2Te_3 , bulk Sb_2Te_3 , bulk Ni, and nanowire composites of Ni were performed and found to be in good agreement with literature values. Based on the test measurements performed with bulk samples of Ni, Bi_2Te_3 , and Sb_2Te_3 , the uncertainty in the measured values is within $1\text{--}2 \mu\text{V/K}$. We also report for the first time the measured values of the Seebeck coefficient for Ni thin films.

Acknowledgment

The authors acknowledge the Department of Mechanical Engineering and Department of Physics and Astronomy at LSU. D.P.Y. acknowledges support from the State of Louisiana Board of Regents (Post Katrina Support Fund, Grant No. 06-719-S4).

References

- [1] Uher, C., 2000, *Semiconductors and Semimetals*, T. M. Tritt, ed., Academic, San Diego, CA, Vol. 69, p. 139.
- [2] Dauscher, A., Lenoir, B., Scherrer, H., and Caillat, T., 2002, *Recent Research Developments in Materials Science*, S. G. Pandala, ed., Research Signpost, Kerala, India, Vol. 3, p. 181.
- [3] *Thermoelectric Handbook, Macro to Nano*, 2006, D. M. Rowe, ed., CRC, Taylor & Francis Group, Boca Raton, FL.
- [4] Ponnambalam, V., Lindsey, S., Hickman, N. S., and Tritt, T. M., 2006, "Sample Probe to Measure Resistivity and Thermopower in the Temperature Range of 300–1000 K," *Rev. Sci. Instrum.*, **77**(7), p. 073904.
- [5] Wood, C., Chmielewski, A., and Zoltan, D., 1988, "Measurement of Seebeck Coefficient Using a Large Thermal Gradient," *Rev. Sci. Instrum.*, **59**(6), pp. 951–954.
- [6] Testardi, L. R., and McConnell, G. K., 1961, "Measurement of the Seebeck Coefficients With Small Temperature Differences," *Rev. Sci. Instrum.*, **32**(9), pp. 1067–1068.
- [7] Cowles, L. E. J., and Dauncey, L. A., 1962, "Apparatus for the Rapid Scanning of the Seebeck Coefficient of Semiconductors," *J. Sci. Instrum.*, **39**(1), pp. 16–18.
- [8] Wood, C., Zoltan, D., and Stapfer, G., 1985, "Measurement of Seebeck Coefficient Using a Light Pulse," *Rev. Sci. Instrum.*, **56**(5), pp. 719–722.
- [9] Caskey, G. R., Sellmyer, D. J., and Rubin, L. G., 1969, "A Technique for Rapid Measurement of Thermoelectric Power," *Rev. Sci. Instrum.*, **40**(10), pp. 1280–1282.
- [10] Chaussy, J., Guessous, A., and Mazuer, J., 1981, "Simultaneous Measurements of Thermopower, Thermal Conductivity, and Electrical Resistivity Between 1.2 and 350 K," *Rev. Sci. Instrum.*, **52**(11), pp. 1721–1731.
- [11] Gee, W., and Green, M., 1970, "An Improved Hot Probe Apparatus for the Measurement of Seebeck Coefficient," *J. Phys. E*, **3**, pp. 135–136.
- [12] Goldsmid, H. J., 1986, "A Simple Technique for Determining the Seebeck Coefficient of Thermoelectrical Materials," *J. Phys. E*, **19**(11), pp. 921–922.
- [13] Platzek, D., Karpinski, G., Stiewe, C., Ziolkowski, P., Draser, C., and Muller, E., 2005, "Potential-Seebeck-Microprobe (PSM): Measuring the Spatial Resolution of the Seebeck Coefficient and the Electrical Potential," *International Conference on Thermoelectrics*, pp. 13–16.
- [14] Pope, A. L., Littleton, R. T., and Tritt, T. M., 2001, "Apparatus for the Rapid Measurement of Electrical Transport Properties for Both Needle-Like and Bulk Materials," *Rev. Sci. Instrum.*, **72**(7), pp. 3129–3131.
- [15] Zhou, Z., and Uher, C., 2005, "Apparatus for Seebeck Coefficient and Electrical Resistivity Measurements of Bulk Thermoelectric Materials at High Temperature," *Rev. Sci. Instrum.*, **76**(2), p. 023901.
- [16] Stolzer, M., Bechstein, V., and Meusel, J., 1998, *Proceedings of the 4th European Workshop on Thermoelectrics*, Madrid, Spain, p. 97.
- [17] Hicks, L. D., and Dresselhaus, M. S., 1993, "Thermoelectric Figure of Merit of a One-Dimensional Conductor," *Phys. Rev. B*, **47**(24), pp. 16631–16634.
- [18] Heremans, J., and Thrush, C. M., 1999, "Thermoelectric Power of Bismuth Nanowires," *Phys. Rev. B*, **59**(19), pp. 12579–12583.
- [19] Dresselhaus, M. S., Dresselhaus, G., Sun, X., Zhang, Z., Cronin, S. B., Koga, T., Ying, J. Y., and Chen, G., 1999, "The Promise of Low Dimensional Thermoelectric Materials," *Nanoscale Microscale Thermophys. Eng.*, **3**(2), pp. 89–100.
- [20] Venkatasubramanian, R., Siivols, E., Colpitts, T., and O'Quinn, B., 2001, "Thin-Film Thermoelectric Devices With High Room-Temperatures Figures of Merit," *Nature (London)*, **413**(6856), pp. 597–602.
- [21] Burkov, A. T., Heinrich, A., Konstantinov, P. P., Nakama, T., and Yagasaki, K., 2001, "Experimental Setup for Thermopower and Resistivity Measurements at 100–1300 K," *Meas. Sci. Technol.*, **12**(3), pp. 264–272.
- [22] Boffoue, O., Jacquot, A., Dauscher, A., Lenoir, B., and Stolzer, M., 2005, "Experimental Setup for the Measurement of the Electrical Resistivity and Thermopower of Thin Films and Bulk Materials," *Rev. Sci. Instrum.*, **76**(5), p. 053907.

- [23] Sarath Kumar, S. R., and Kasiviswanathan, S., 2008, "A Hot Probe Setup for the Measurement of Seebeck Coefficient of Thin Wires and Thin Films Using Integral Method," *Rev. Sci. Instrum.*, **79**(2), p. 024302.
- [24] Ren, Z. A., Che, G. C., Jia, S. L., Chen, H., Ni, Y. M., Liu, G. D., and Zhao, Z. X., 2002, "The Structural Change and Superconductivity in MgC_xNi_3 ($x=0.5-1.55$) and $\text{Mg}_x\text{C}_y\text{Ni}_3$ ($x=0.75-1.55$, $y=0.85$, 1 and 1.45) and the Phase Diagram of Ni Rich Region in Mg-C-Ni Ternary System," *Physica C*, **371**(1), pp. 1-6.
- [25] Jackson, D. D., McCall, S. K., Weir, S. T., Karki, A. B., Young, D. P., Qiu, W., and Vohra, Y. K., 2007, "Cubic Laves Ferromagnet TbNi_2Mn Investigated Through Ambient-Pressure Magnetization and Specific Heat and High Pressure AC Magnetic Susceptibility," *Phys. Rev. B*, **75**(22), p. 224422.
- [26] Schönenberger, C., van der Zande, B. M. I., Fokink, L. G. J., Henny, M., Schmid, C., Krüger, M., Bachtold, A., Huber, R., Birk, H., and Staufer, U., 1997, "Template Synthesis of Nanowires in Porous Polycarbonate Membranes: Electrochemistry and Morphology," *J. Phys. Chem. B*, **101**(28), pp. 5497-5505.
- [27] Ferré, R., Ounadjela, K., George, J. M., Piraux, L., and Dubois, S., 1997, "Magnetization Processes in Nickel and Cobalt Electrodeposited Nanowires," *Phys. Rev. B*, **56**(21), pp. 14066-14075.
- [28] Nielsch, K., Müller, F., Li, A. P., and Gosele, U., 2000, "Uniform Nickel Deposition Into Ordered Alumina Pores by Pulsed Electrodeposition," *Adv. Mater.*, **12**(8), pp. 582-586.
- [29] Pignard, S., Goglio, G., Radulescu, A., Piraux, L., Dubois, S., Declémy, A., and Duvaill, J. L., 2000, "Study of Magnetization Reversal in Individual Nickel Nanowires," *J. Appl. Phys.*, **87**(2), pp. 824-829.
- [30] Sellmyer, D. J., Zheng, M., and Skomski, R., 2001, "Magnetism of Fe, Co and Ni Nanowires in Self-Assembled Arrays," *J. Phys.: Condens. Matter*, **13**(25), pp. R433-R460.
- [31] Jin, C. G., Liu, W. F., Jia, C., Xiang, X. Q., Cai, W. L., Yao, L. Z., and Li, X. G., 2003, "High-Filling, Large-Area Ni Nanowire Arrays and the Magnetic Properties," *J. Cryst. Growth*, **258**(3-4), pp. 337-341.
- [32] Pan, H., Liu, B., Yi, J., Poh, C., Lim, S., Ding, J., Feng, Y., Huan, C. H. A., and Lin, J., 2005, "Growth of Single-Crystalline Ni and Co Nanowires via Electrochemical Deposition and Their Magnetic Properties," *J. Phys. Chem. B*, **109**(8), pp. 3094-3098.
- [33] Wen, S., and Szpunar, J. A., 2006, "Direct Electrodeposition of Highly Ordered Magnetic Nickel Nanowires," *Micro & Nano Lett.*, **1**(2), pp. 89-93.
- [34] Xue, S., Cao, C., and Zhu, H., 2006, "Electrochemically and Template-Synthesized Nickel Nanorod Arrays and Nanotubes," *J. Mater. Sci.*, **41**(17), pp. 5598-5601.
- [35] Tian, F., Zhu, J., and Wei, D., 2007, "Fabrication and Magnetism of Radial-Easy-Magnetized Ni Nanowire Arrays," *J. Phys. Chem. C*, **111**(34), pp. 12669-12672.
- [36] Ertan, A., Tewari, S. N., and Talu, O., 2008, "Electrodeposition of Nickel Nanowires and Nanotubes Using Various Templates," *J. Exp. Nanosci.*, **3**(4), pp. 287-295.
- [37] Imran, M. M. A., 2008, "Structural and Magnetic Properties of Electrodeposited Ni Nanowires," *J. Alloys Compd.*, **455**(1-2), pp. 17-20.
- [38] Shi, J. B., Chen, Y. C., Lee, C. W., Lin, Y. T., Wu, C., and Chen, C. J., 2008, "Optical and Magnetic Properties of 30 and 60 nm Ni Nanowires," *Mater. Lett.*, **62**(1), pp. 15-18.
- [39] Li, X., Wang, Y., Song, G., Peng, Z., Yu, Y., She, X., and Li, J., 2009, "Synthesis and Growth Mechanisms of Ni Nanotubes and Nanowires," *Nanoscale Res. Lett.*, **4**, pp. 1015-1020.
- [40] Martin, C. R., 1996, "Membrane-Based Synthesis of Nanomaterials," *Chem. Mater.*, **8**(8), pp. 1739-1746.
- [41] Kline, T. R., Tian, M., Wang, J., Sen, A., Chan, M. W. H., and Mallouk, T. E., 2006, "Template-Grown Metal Nanowires," *Inorg. Chem.*, **45**(19), pp. 7555-7565.
- [42] Zhitinskaya, M. K., Nemov, S. A., and Ivanova, L. D., 2002, "The Nernst-Ettingshausen, Seebeck and Hall Effects in Sb_2Te_3 Single Crystals," *Phys. Solid State*, **44**(1), pp. 42-47.
- [43] Lowhorn, N. D., Wong-Ng, W., Zhang, W., Lu, Z. Q., Otani, M., Thomas, E., Green, M., Tran, T. N., Dilley, N., Ghamaty, S., Elsner, N., Hogan, T., Downey, A. D., Jie, Q., Li, Q., Obara, H., Sharp, J., Caylor, C., Venkatasubramanian, R., Willigun, R., Yang, J., Martin, J., Nolas, G., Edwards, B., and Tritt, T., 2009, "Round-Robin Measurements of Two Candidate Materials for a Seebeck Coefficient Standard Reference Materials," *Appl. Phys. A: Mater. Sci. Process.*, **94**, pp. 231-234.
- [44] Blatt, F. J., Flood, D. J., Rowe, V., and Schroeder, P. A., 1967, "Magnon-Drift Thermopower in Iron," *Phys. Rev. Lett.*, **18**(11), pp. 395-396.
- [45] Shapira, E., Tsukernik, A., and Selzer, Y., 2007, "Thermopower Measurements on Individual 30 nm Nickel Nanowires," *Nanotechnology*, **18**(48), p. 485703.
- [46] Soni, A., and Okram, G. S., 2009, "Size-Dependent Thermopower in Nanocrystalline Nickel," *Appl. Phys. Lett.*, **95**(1), p. 013101.